Scientific Research Report

Fusobacterium nucleatum-Derived Outer Membrane Vesicles Disrupt Epithelial Barrier in Oral Lichen Planus via JNK/c-JUN Mediated Claudin-4 Downregulation

Ruru Shao [a,#], *Zhenyuan Wang* [b,#], *Chenglong Yang* [b], *Junjun Chen* [a*], *Guanhuan Du* [a*]

[a] *Department of Oral Mucosal Diseases, Shanghai Ninth People's Hospital, Shanghai Jiao Tong University School of Medicine; College of Stomatology, Shanghai Jiao Tong University, National Center for Stomatology;National Clinical Research Center for Oral Diseases;Shanghai Key Laboratory of Stomatology; Shanghai Research Institute of Stomatology, Shanghai, China*

[b] *Department of Stomatology, Xinhua Hospital, Shanghai Jiao Tong University School of Medicine, Core Unit of National Clinical Research Center for Oral Diseases, Shanghai, China*

ARTICLE INFO

Article history:
Received 2 December 2025
Received in revised form
26 February 2026
Accepted 3 March 2026
Available online xxx

Key words:
Oral lichen planus
Fusobacterium nucleatum
Outer membrane vesicles
Claudin-4

ABSTRACT

Introduction and aims: Oral lichen planus (OLP) is a chronic inflammatory disease of unknown etiology. Recent studies have implicated microbial dysbiosis in its pathogenesis. Our previous research revealed an increased abundance of *Fusobacterium nucleatum* (*F.nucleatum*) in OLP tissues, suggesting its potential involvement.

Methods: We utilized single-cell RNA sequencing, spatial transcriptomics, and immunohistochemistry to analyse Claudin-4 expression and its spatial distribution in OLP lesions. In vitro, HaCaT keratinocytes exposed to outer membrane vesicles (OMVs) derived from *F.nucleatum* (*F.n*-OMVs) were evaluated for epithelial barrier function via transepithelial electrical resistance (TEER) and fluorescein isothiocyanate-dextran (FD4) permeability assays. Claudin-4 expression and JNK/c-JUN pathway activation were evaluated by qPCR, Western blotting, and RNA sequencing. The JNK inhibitor SP600125 was used to explore pathway involvement.

Results: Claudin-4 expression was significantly decreased and exhibited disrupted spatial organization in OLP lesions. *F.n*-OMVs compromised HaCaT epithelial barrier function, downregulated Claudin-4 expression, and altered its localization. Western blotting demonstrated activation of the JNK/c-JUN signaling pathway. Inhibition of JNK with SP600125 restored Claudin-4 expression and barrier function.

Conclusion: Our study demonstrates that *F.n*-OMVs induce epithelial barrier dysfunction in OLP by activating the JNK/c-JUN pathway to downregulate Claudin-4, highlighting a novel microbial mechanism contributing to OLP pathogenesis.

Clinical Relevance: These findings identify *F.n*-OMVs as microbial drivers of epithelial barrier disruption in OLP, suggesting that targeting OMVs or the JNK/c-JUN/Claudin-4 axis may offer new diagnostic and therapeutic strategies for OLP management.

* *Corresponding authors*. Department of Oral Mucosal Diseases, Shanghai Ninth People's Hospital, Shanghai Jiao Tong University School of Medicine, No. 500, Quxi Road, Huangpu District, Shanghai 200011, China.
E-mail addresses: 2008chenjunjun@163.com (J. Chen), dgh-09@163.com (G. Du).
Guanhuan Du: http://orcid.org/0000-0002-5565-8657

# Ruru Shao and Zhenyuan Wang contributed equally to this work and share first authorship.

https://doi.org/10.1016/j.identj.2026.109526

Introduction

Oral lichen planus (OLP) is a chronic inflammatory disease of the oral mucosa characterized by T cell-mediated immune responses, and its pathogenesis remains incompletely understood.[1] Traditional perspectives have primarily focused on endogenous factors such as host immune dysregulation, genetic susceptibility, and psychological stress.[2] However, with the advancement of microbial ecology, accumulating evidence suggests that local dysbiosis of the oral mucosal microbiota may play a pivotal pathogenic role in the initiation and progression of OLP.[3]

In recent years, multiple high-throughput sequencing studies have suggested that the composition of the oral microbiota is significantly altered in patients with OLP.[4-6] Our previous metagenomic sequencing further revealed a marked enrichment of *Fusobacterium nucleatum* (*F.nucleatum*) in the saliva and lesional tissues of OLP patients compared to healthy controls, with a significantly higher relative abundance, suggesting a potential pathogenic role of this bacterium in the onset and progression of OLP.[7]

Fusobacteria are Gram-negative anaerobic bacilli that inhabit distinct ecological niches within the human body, including the oral cavity, gastrointestinal tract, and other mucosal surfaces.[8] Outer membrane vesicles (OMVs) are nanoscale, spherical bilayered structures released from the outer membrane of Gram-negative bacteria. They are enriched with a variety of immunogenic components—including lipopolysaccharide (LPS), flagellin, and peptidoglycan—that can potently activate the host immune system, primarily through engagement with Toll-like receptors (TLRs).[9]

Recent studies have demonstrated that OMVs released by *F.nucleatum* (*F.n*-OMVs) play an important role in the initiation and progression of various diseases, including colorectal cancer, ulcerative colitis, and rheumatoid arthritis.[10-12] In oral diseases, especially chronic inflammatory diseases and tumour-related diseases, such as periodontitis and oral squamous cell carcinoma, *F.n*-OMVs also show significant pathogenic potential.[13-14] However, most existing studies have predominantly focused on immune activation and inflammatory outcomes, while the direct effects of *F.n*-OMVs on oral epithelial barrier integrity and tight junction regulation remains largely unexplored.

The oral mucosal epithelial barrier plays a pivotal role in defending against microbial invasion and toxic insults, and its structural and functional integrity is essential for maintaining mucosal homeostasis.[15] Previous studies have confirmed the presence of abundant bacteria within both the epithelial and lamina propria layers of OLP tissues, and certain oral microbial species have been shown to disrupt the physical epithelial barrier and internalize into epithelial cells.[16] Our in-depth analysis of single-cell transcriptomic data from OLP tissues revealed a significant downregulation of the tight junction protein Claudin-4 in lesional epithelial cells.[17] Notably, this observation provides epithelial cell specific and spatially resolved transcriptional evidence at single-cell resolution, extending previous bulk-level findings. Consistently, other researchers have also reported decreased expression levels of Claudin-1, Claudin-4, and E-cadherin in OLP tissues.[18] Nevertheless, these studies were largely descriptive and did not address the upstream microbial drivers or intracellular signalling mechanisms underlying tight junction dysregulation. As a member of the claudin family, Claudin-4 plays a crucial role in maintaining epithelial barrier function, and its aberrant expression or mislocalization may compromise epithelial integrity, suggesting its potential involvement in the pathogenesis of OLP.[19] Despite accumulating evidence linking epithelial barrier impairment to tight junction downregulation in OLP, the specific microbial factors responsible for this process and the host signalling pathways involved remain unclear. In particular, whether *F.n*-OMVs directly interfere with tight junction architecture through defined intracellular signalling cascades has not been elucidated.

Therefore, this study aimed to investigate whether *F.n*-OMVs contribute to oral epithelial barrier disruption by regulating Claudin-4 expression. By integrating single-cell and spatial transcriptomic analyses with in vitro epithelial cell models, we demonstrate that *F.n*-OMVs induce Claudin-4 downregulation and barrier dysfunction through activation of the JNK/c-JUN signalling pathway. These findings identify a previously unrecognized mechanistic link between microbial-derived OMVs and epithelial tight junction regulation in OLP, providing new insights into disease pathogenesis and potential therapeutic targets for preserving epithelial barrier integrity.

Materials and methods

Single-cell RNA sequencing data analysis

Single-cell RNA sequencing (scRNA-seq) data of oral mucosal tissues from patients with oral lichen planus and healthy controls were obtained from the public database (https://www.ncbi.nlm.nih.gov/geo/) under accession number GSE211630. Raw gene expression matrices were processed and analysed using the Seurat package (v5.2.1) in R (version 4.4.1). Low-quality cells were filtered out based on the following criteria: fewer than 300 detected genes, fewer than 1,000 total unique molecular identifiers (UMIs), or mitochondrial gene expression exceeding 20% of total counts. Highly variable genes were identified using the FindVariableFeatures function (top 2,000 genes). Batch correction and integration of multiple samples were performed using the Harmony algorithm to eliminate batch effects. The integrated data were scaled using the ScaleData function to normalize expression levels and remove unwanted variation. Dimensionality reduction was performed via principal component analysis (PCA) using RunPCA, followed by clustering with the FindNeighbors and FindClusters functions based on cell–cell similarity. Nonlinear dimensionality reduction was conducted using Uniform Manifold Approximation and Projection (UMAP) for visualization.

Sample collecting

Human oral mucosal biopsy samples were obtained from patients clinically and histologically diagnosed with oral lichen planus (OLP) at the Ninth People's Hospital, Shanghai Jiao Tong University School of Medicine. Written informed consent was obtained from all participants prior to enrolment. This study was approved by the Ethics Committee of

the Ninth People's Hospital, Shanghai Jiao Tong University School of Medicine (SH9H-2020-T76-2).

Spatial transcriptomics (ST)

ST process

Freshly collected OLP lesion tissue s were dissected into appropriately sized tissue blocks, embedded in OCT Medium (SAKURA, cat.no. 4583), and snap-frozen on dry ice. The embedded tissue samples were stored at -80 °C. Subsequently, the embedded samples were sent to OE Biotech Co., Ltd. for spatial transcriptomic library preparation, sequencing, and data analysis. Briefly, frozen sections of 10 μm thickness were prepared using a Leica CM1950 Microtome Cryostat (Leica Microsystems) at -20°C. Tissue sections were subjected to methanol fixation, HE staining, imaging and destaining following the 10x Genomics recommended experimental procedure (CG000614). According to the 10x Genomics experimental flow (CG000495), probe hybridization, probe release and transferred to the 10x Genomics Visium CytAssist slide, and the library construction was performed using the Visium CytAssist Spatial Gene Expression for FFPE kit (PN-1000520 for Human, 6.5mm). The libraries were were sequenced on the BGI DNBSEQ-T7 sequencing platformusing PE100 mode.

ST analysis

Raw sequencing data were processed using the 10x Genomics Space Ranger pipeline (v2.0.1). The spatial gene expression matrices were further analysed using the Seurat (v4.1.0) in R. Spots with low transcript counts or high mitochondrial gene content were filtered out, and normalization and dimensionality reduction (PCA, UMAP) were performed. Spatial clustering, cell-type deconvolution, and spatial feature plotting were used to identify transcriptional heterogeneity and regional gene expression patterns within the tissue sections.

Histology and immunohistochemistry (IHC)

All tissue samples from OLP patients and healthy controls were fixed in 10% buffered formalin and embedded in paraffin. Immunohistochemistry was performed using standard protocols. The Claudin-4 antibody used for immunohistochemical staining was diluted at 1:100. Images were captured using an Olympus microscope under identical acquisition settings. Quantitative analysis of Claudin-4 expression was performed using ImageJ software by calculating the percentage of positively stained area relative to the total epithelial area.

Cell lines

The human immortalized keratinocyte cell line HaCaT was kindly provided by Professor Guoyao Tang (Xinhua Hospital, Shanghai Jiao Tong University School of Medicine). Cells were maintained in DMEM (Gibco) supplemented with 10% fetal bovine serum (FBS) and 1% penicillin-streptomycin, and incubated at 37°C in a humidified atmosphere containing 5% CO_2.

Bacterial culture and OMVs isolation

F.nucleatum(ATCC® 25586™) was cultured anaerobically at 37° C in an atmosphere containing 99% nitrogen until the optical density at 600 nm reached 1.5, as previously described.[12] The isolation of OMVs was performed as follows.[20] Briefly, bacterial cultures were centrifuged at 3000 rpm for 5 minutes, and the supernatants were collected and passed through a 0.22 μm filter to eliminate residual bacterial fragments and impurities. A 300 kDa molecular weight cut-off dialysis membrane (Spectrum Labs, USA) was used for vesicle isolation. Electrophoretic buffer was prepared with deionized water containing glycine (7.2 g/L) and Tris base (1.5 g/L), both obtained from Sangon Biotech. A 5 mL aliquot of the filtered supernatant was sealed inside the dialysis membrane using Parafilm. The sealed bag was placed into a western blot transfer cassette, and electrophoresis was performed at a constant current of 300 mA to isolate OMVs. After 30 minutes, the buffer was replaced and the polarity was reversed. OMVs were harvested after 2 hours of continuous electrophoretic separation. The particle size and morphology of the OMVs were characterized and analysed by using nanoparticle tracking analysis (NTA) and transmission electron microscopy (TEM).

Treatment of HaCaT cells with F.n-OMVs

To determine appropriate experimental conditions, HaCaT cells were initially treated with increasing concentrations of *F.n*-OMVs (0, 1, 2, 5, and 10 μg/mL) for different durations (6, 12, 18, and 24h). Transepithelial electrical resistance (TEER) was measured to evaluate time- and dose-dependent effects on epithelial barrier integrity. The most pronounced barrier disruption was observed at 24 h.

Based on this time point, HaCaT cells were subsequently treated with the same range of *F.n*-OMVs concentrations for 24 h. Epithelial permeability was assessed using FITC-dextran assays, and Claudin-4 expression was analysed by RT-qPCR and Western blotting. Treatment with 10 μg/mL *F.n*-OMVs for 24 h induced the most significant barrier dysfunction and Claudin-4 downregulation.

Accordingly, 10μg/mL *F.n*-OMVs for 24 h was selected for all subsequent experiments, including immunofluorescence staining, RNA sequencing, and mechanistic studies involving JNK pathway inhibition.

Evaluation of paracellular permeability using FITC-dextran

HaCaT cells were seeded into the upper compartments of Transwell inserts placed in 6-well plates and cultured until a continuous monolayer was established. A solution of fluorescein isothiocyanate-conjugated dextran (4kDa, 1 mg/mL; Sigma) prepared in PBS was gently added to the apical side. After incubation at 37°C for 2 hours, medium was collected from the basolateral chamber. The fluorescence intensity (excitation at 485 nm and emission at 525 nm) was quantified using a microplate reader (Thermo, USA) to determine the extent of FITC-dextran translocation, which reflects epithelial barrier integrity.

Assessment of transepithelial electrical resistance (TEER)

HaCaT cells were seeded onto Transwell inserts and cultured until a confluent monolayer was formed. Cells were treated with increasing concentrations of *F.n*-OMVs for the indicated durations. TEER was measured using the Millicell-ERS system (Millipore, USA) under constant temperature conditions. Blank controls consisted of two Transwell inserts containing only culture medium without cells. Resistance was recorded at three different positions per insert and repeated three times per position, with the mean value used for final calculation. TEER values ($\Omega \cdot cm^2$) were obtained by subtracting the resistance of the blank insert from the measured value and multiplying by the surface area of the insert membrane, as per the formula: TEER = (Measured resistance − Blank resistance) × Membrane area.

RNA extraction and quantitative Real-Time PCR (RT-qPCR)

Total RNA was extracted from HaCaT cells treated with *F.n*-OMVs for 24 hours using TRIzol reagent according to the manufacturer's instructions, including phase separation with chloroform, RNA precipitation with isopropanol, and ethanol washing. For pathway inhibition experiments, cells were pretreated with the JNK inhibitor SP600125 (10 μM) for 1 hour prior to OMV stimulation (10 μg/mL for 24 hours). Reverse transcription was performed using a reverse transcriptase kit (Takara, Japan). The subsequent quantitative real-time PCR amplification was performed with SYBR Green Premix ExTaq (Takara, Japan) using the Step-One plus System. The cycling conditions were as follows: initial denaturation at 95°C for 30 seconds, followed by 40 cycles of denaturation at 95°C for 5 seconds and annealing/extension at 60°C for 30 seconds. Relative mRNA expression levels were calculated using the $2^{-\Delta\Delta CT}$ method, with GAPDH as the internal control.

The gene-specific primer sequences are listed in Table 1.

Western blot

Cells were lysed using RIPA buffer, and the supernatant was collected. Protein concentration was determined using the BCA assay. Equal amounts of protein (20 μg) were separated by 12.5% SDS-PAGE and transferred onto PVDF membranes. The membranes were blocked with a serum-free rapid blocking solution at room temperature for 1 hour, followed by overnight incubation at 4°C with the following primary antibodies diluted 1:1000 in blocking buffer: anti-Claudin-4 (ab53156, Abcam), anti-GAPDH (clone D16H11, CST), anti-JNK (ab208035, Abcam), anti-c-JUN (ab31419, Abcam), anti-phospho-JNK (Thr183/Tyr185, clone81E11, CST), and anti-phospho-c-JUN (Ser73, ab31419,Abcam). After washing with TBST, membranes were incubated for 1h at room temperature with horseradish peroxidase (HRP)-conjugated secondary antibodies, including goat anti-rabbit IgG-HRP and goat anti-mouse IgG-HRP (both 1:5000; Yamay Biotechnology). Protein bands were visualized using an enhanced chemiluminescence (ECL) detection reagent and imaged using a Tanon chemiluminescence imaging system (Tanon Science & Technology Co., Ltd., Shanghai).

Immunocytochemistry

HaCaT cells (1×10^5 cells/well) were seeded onto glass coverslips in 24-well plates. After adherence, cells were treated with OMVs derived from *F.nucleatum* at a concentration of 10ug/mL for 24 hours. Following treatment, cells were washed with pre-chilled PBS and fixed with 4% paraformaldehyde for 15 minutes. After fixation, cells were blocked with blocking solution containing Triton X-100 for 1 hour at room temperature. The blocking solution was removed, and the cells were incubated overnight at 4°C with a primary antibody against Claudin-4 (1:200 dilution). The next day, cells were incubated with Alexa Fluor 488-conjugated secondary antibody (1:500 dilution), counterstained with DAPI-containing mounting medium, and observed under an inverted fluorescence microscope.

RNA-sequencing (RNA-seq)

Total RNA for RNA-sequencing was extracted from control and *F.n*-OMVs-treated HaCaT cells (10 μg/mL for 24 hours) using TRIzol reagent. High-throughput RNA sequencing was performed on the Illumina NovaSeq 6000 platform, following standard protocols. Raw sequencing data quality was assessed using FastQC. Differential gene expression analysis between *F.n*-OMVs-treated and control groups was conducted using the DESeq2 package in R. Genes with an absolute log2 fold change ($|log2FC| \geq 1$ and an adjusted *P*-value ≤ 0.05 were considered significantly differentially expressed genes (DEGs). To explore the biological functions of DEGs, Kyoto Encyclopedia of Genes and Genomes (KEGG) pathway enrichment analysis was performed using the "ClusterProfiler" R package. The raw and processed RNA-seq data generated in this study have been deposited in the Gene Expression Omnibus (GEO) under accession number GSE320506.

Statistical analysis

Statistical analysis was conducted using GraphPad Prism version 8.0. Data are presented as mean values with corresponding standard deviations (mean ± SD). Comparisons between two groups were assessed using the unpaired Student's t-test, while differences among more than two groups were

Table 1 – Primer sequences used for RT-qPCR experiments.

	Forward primer (5'-3')	Reverse primer (5'-3')
GAPDH	GAAGGTGAAGGTCGGAGTC	GAAGATGGTGATGGGATTTC
CLDN4	TGGGGCTACAGGTAATGGG	GGTCTGCGAGGTGACAATGTT

evaluated through one-way ANOVA followed by Tukey's multiple comparisons test. All experiments were independently repeated at least three times. A *P*-value of less than 0.05 was considered to indicate a statistically significant difference.

Results

Claudin-4 is significantly downregulated in OLP tissues

We analysed single-cell transcriptomic data from human buccal mucosal tissue and found that Claudin-4 was primarily localized in the epithelial cell subpopulation, with a decreased expression trend observed in the buccal mucosa of patients with OLP (Figure 1A-D) . Immunohistochemical analysis further confirmed that Claudin-4 expression was significantly reduced in OLP tissues compared to healthy controls (Figure 1E, F). These findings suggest that Claudin-4 may play a critical role in the pathogenesis of oral lichen planus.

Spatial transcriptomic analysis reveals epithelial barrier dysfunction associated with Claudin-4 downregulation in oral lichen planus

To investigate the spatial distribution of Claudin-4 expression in OLP, we performed spatial transcriptomic profiling on buccal mucosa tissues from healthy controls (n = 8) and OLP patients (n = 7). In healthy samples, Claudin-4 expression was consistently high and localized predominantly within the epithelial regions, forming continuous expression zones (Figure 2A).

In contrast, OLP samples showed markedly decreased Claudin-4 expression. Most OLP tissues displayed patchy or near-complete loss of Claudin-4 signal in areas corresponding to epithelial disruption (Figure 2B). These spatially resolved differences indicate that the downregulation of Claudin-4 is regionally confined and correlates with epithelial structural disorganization in OLP tissues.

Characterization of F.n-OMVs

TEM revealed that *F.n*-OMVs were structurally intact and exhibited a characteristic cup-shaped morphology (Figure 3A). NTA showed that the particle size of these OMVs was primarily distributed around 100 nm, consistent with the TEM observations (Figure 3B). These purified OMVs were subsequently used in downstream experimental assays.

F.n-OMVs *disrupt epithelial barrier function in HaCaT cells and downregulate Claudin-4 expression*

To evaluate the impact of *F.n*-OMVs on epithelial barrier function, HaCaT cells were treated with increasing concentrations of OMVs (0, 1, 2, 5, and 10 μg/mL) for various durations (6, 12, 18, and 24 hours), followed by measurement of TEER. The results revealed a time- and dose-dependent reduction in TEER values, suggesting progressive epithelial barrier impairment, with the most substantial decrease observed at 24 hours (Figure 3C). Furthermore, treatment of HaCaT cells with different concentrations of OMVs for 24 hours resulted in significantly increased FITC-dextran permeability (Figure 3D), providing additional evidence of compromised epithelial barrier integrity.

At the molecular level, qPCR and Western blot analyses revealed a marked downregulation of Claudin-4 mRNA and protein expression following OMV treatment in a dose-dependent manner (Figure 3E, 3F). Based on these results, treatment with 10 μg/mL OMVs for 24 hours was selected as the optimal condition for subsequent mechanistic studies.

Additionally, immunofluorescence staining further confirmed these findings. In the *F.n*-OMVs treated group, Claudin-4 fluorescence intensity was markedly reduced and displayed a discontinuous membrane distribution, suggesting altered expression and localization. (Figure 3G).

Taken together, these results indicate that *F.n*-OMVs can significantly impair the structural and functional integrity of the epithelial barrier in HaCaT cells by downregulating the tight junction protein Claudin-4.

Multi-omics reveals the key role of the MAPK signalling pathway in barrier disruption mediated by F.n-OMVs

To further investigate the underlying mechanism by which *F.n*-OMVs impair keratinocyte barrier function, we performed transcriptomic analysis on HaCaT cells treated with *F.n*-OMVs for 24 hours. Differentially expressed genes (DEGs) were identified and subjected to bioinformatic analysis (Figure 4A). KEGG pathway enrichment analysis revealed that several signalling pathways closely associated with epithelial barrier homeostasis were significantly affected. Among them, the MAPK signalling pathway was the most significantly enriched (Figure 4B), suggesting that it may play a key role in OMVs-induced barrier disruption and downregulation of Claudin-4 expression.

Further examination of the RNA-seq data showed that multiple key regulatory components of the MAPK pathway—including MAP3K21, MAP3K9, JUN, and FOS—were markedly upregulated, while tight junction-related genes such as Claudin-7, Claudin-4, and Claudin-1 were significantly downregulated (Figure 4C). These results imply that activation of the MAPK pathway may mediate the repression of tight junction genes. To validate this trend, we analysed single-cell RNA sequencing data, which revealed that JUN expression was elevated across multiple epithelial cell subsets(Figure 4D,E). Additionally, spatial transcriptomic analysis also demonstrated significant enrichment of the MAPK signalling pathway in the *F.n*-OMVs-treated group, further supporting the involvement of this pathway in OMVs-induced barrier impairment(Figure 4G,F).

Collectively, our integrated multi-omics analysis suggests that *F.n*-OMVs may disrupt epithelial barrier function by activating the MAPK signalling pathway, which in turn downregulates the expression of tight junction proteins.

The JNK/c-JUN pathway plays a critical role in F.n-OMVs *induced downregulation of Claudin-4*

To further investigate the role of the JNK/c-JUN signalling pathway in the *F.n*-OMVs induced disruption of epithelial barrier function, we treated HaCaT cells with the specific JNK inhibitor SP600125. Cells were divided into four groups:

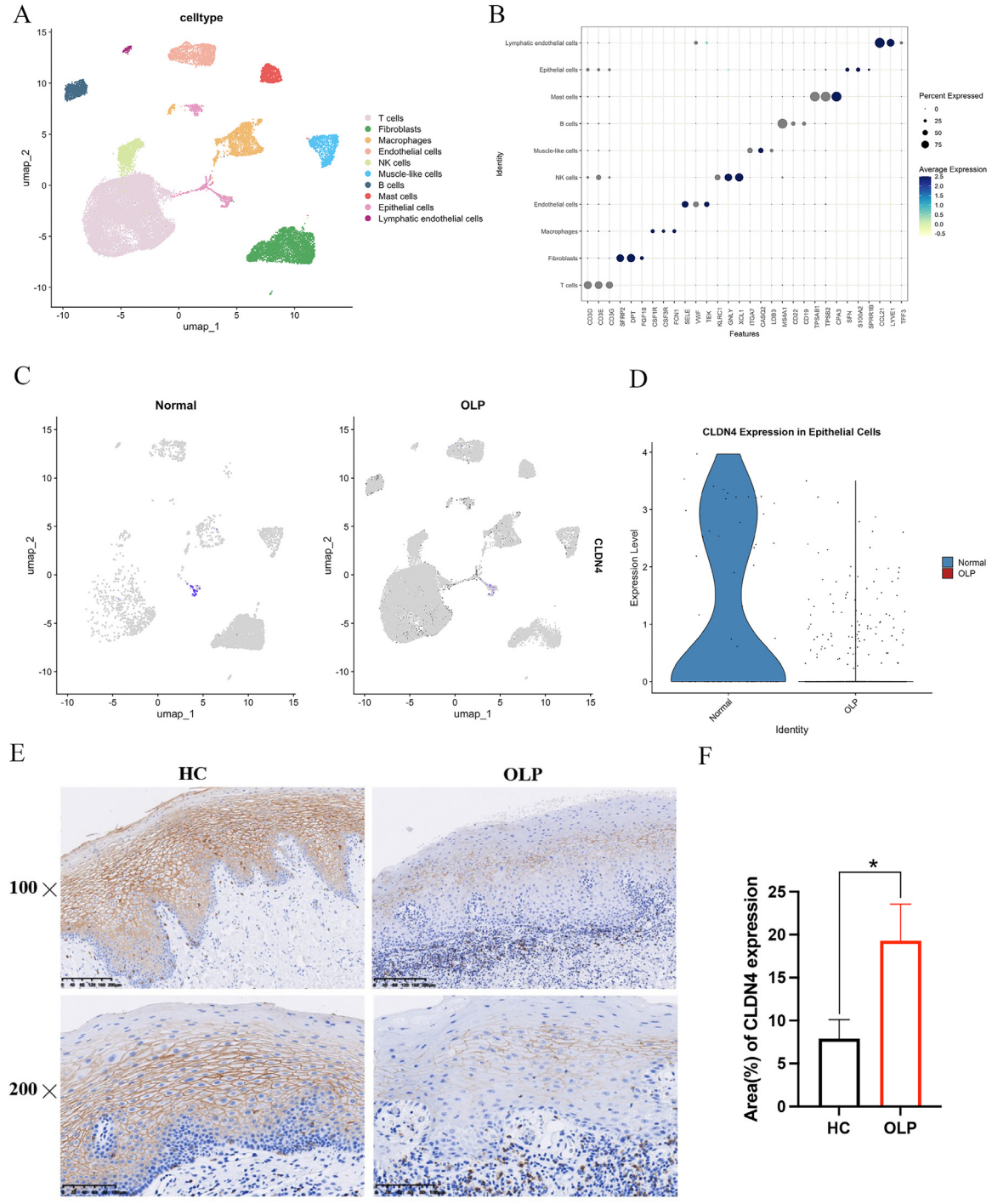

Fig. 1 – Single-cell transcriptomic and immunohistochemical analysis of Claudin-4 expression in oral mucosal tissues. (A) UMAP plot showing cell clustering from scRNA -seq data of oral mucosal samples. Each cluster represents a distinct cell population. (B) Dot plot showing the expression of selected marker genes across different cell clusters. (C) Feature plot visualizing the spatial expression pattern of Claudin-4 on the UMAP projection. (D) Violin plot showing the differential expression of Claudin-4 specifically in epithelial cells between healthy controls (HC) and oral lichen planus (OLP) patients. (E) Representative immunohistochemistry (IHC) staining of Claudin-4 in oral epithelial tissues from HC and OLP patients. Images are shown at 100 × and 200 × magnification. (F) Quantitative analysis of Claudin-4 IHC staining, expressed as the percentage of Claudin-4 positive expression area within the epithelial region. *$p < 0.05$.

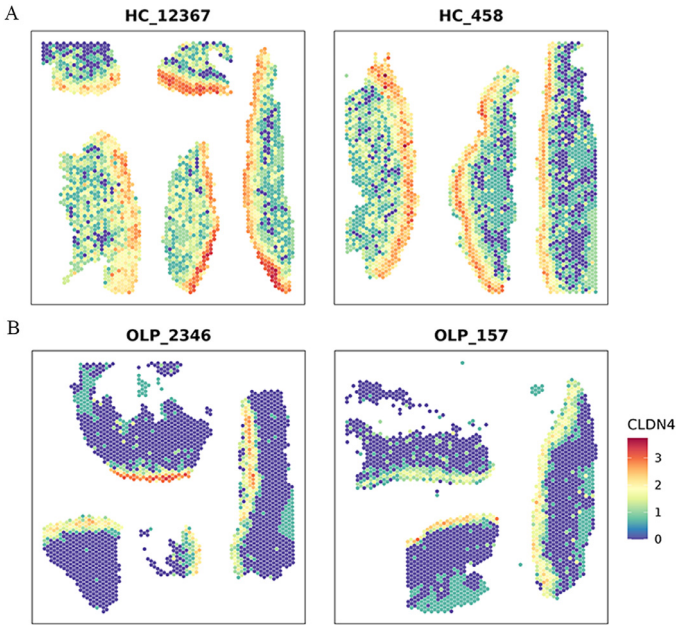

Fig. 2 – Spatial expression patterns of CLDN4 in oral mucosal tissues from healthy controls and OLP patients. (A) Representative spatial transcriptomics maps showing CLDN4 expression in oral mucosal tissues from healthy controls (HC_12367 and HC_458). (B) Representative spatial transcriptomics maps showing CLDN4 expression in tissues from OLP patients (OLP_2346 and OLP_157).Each dot represents a spatially resolved transcriptomic spot, colored by normalized expression levels of CLDN4 (color scale: blue = low, red = high).

Control, OMVs (10 μg/mL for 24 h), SP600125 alone (10 μM pretreatment for 1 h), and OMVs combined with SP600125. qPCR analysis revealed that treatment with *F.n*-OMVs significantly reduced Claudin-4 mRNA expression, whereas pretreatment with SP600125 markedly reversed this downregulation, suggesting that activation of the JNK pathway contributes to the transcriptional repression of Claudin-4 (Figure 5A). Consistently, Western blot analysis demonstrated that Claudin-4 protein levels were significantly reduced after OMVs stimulation but were restored to near-baseline levels following SP600125 pretreatment (Figure 5B).

To confirm the inhibition of the signalling pathway, we assessed the phosphorylation levels of JNK and its downstream transcription factor c-JUN. OMVs stimulation led to a pronounced increase in p-JNK and p-c-JUN expression, indicating robust pathway activation. In contrast, SP600125 treatment significantly decreased the phosphorylation levels of both JNK and c-JUN, confirming effective inhibition of the pathway (Figure 5B).

Collectively, these findings suggest that *F.n*-OMVs downregulate CLDN4 expression through activation of the JNK/c-JUN signalling pathway, contributing to epithelial barrier disruption (Figure 6). Notably, pharmacological inhibition of this pathway by SP600125 effectively restored Claudin-4 expression, underscoring the central regulatory role of JNK/c-JUN in OMVs-mediated barrier impairment.

Discussion

In this study, we demonstrated that *F.n*-OMVs significantly impair oral epithelial barrier integrity by downregulating the expression of the tight junction protein Claudin-4 via activation of the JNK/c-JUN signalling pathway. Using an integrated approach combining in vitro experiments with spatial and single-cell transcriptomics, we revealed that Claudin-4 is markedly decreased in the epithelial compartments of OLP lesions, while JNK pathway components such as JUN are significantly upregulated. Functional assays showed that *F.n*-OMVs reduce transepithelial electrical resistance and increase epithelial permeability, consistent with tight junction disruption. Notably, pharmacological inhibition of JNK signalling restored Claudin-4 expression and partially rescued epithelial barrier function. Together, these findings extend previous descriptive observations by providing direct mechanistic evidence linking microbial-derived OMVs to epithelial barrier dysfunction through a defined intracellular signalling pathway. Our findings uncover a novel mechanism by which *F.n*- OMVs contribute to epithelial barrier dysfunction in OLP, providing mechanistic insight into how microbial dysbiosis may drive mucosal inflammation and disease progression.

Previous studies have repeatedly reported significant epithelial barrier dysfunction in patients with OLP, which is closely associated with the downregulation of multiple tight junction proteins. It has been found that the expression levels of Claudin-1, Claudin-4, Occludin, and Zonula Occludens-1 (ZO-1) are significantly reduced in OLP tissues, suggesting that these key tight junction proteins play an important role in maintaining the integrity of the oral mucosal barrier.[21] Additionally, another study reported that the expression levels of Claudin-1, Claudin-4, and E-cadherin are significantly reduced in the epithelium of OLP patients,[18] further

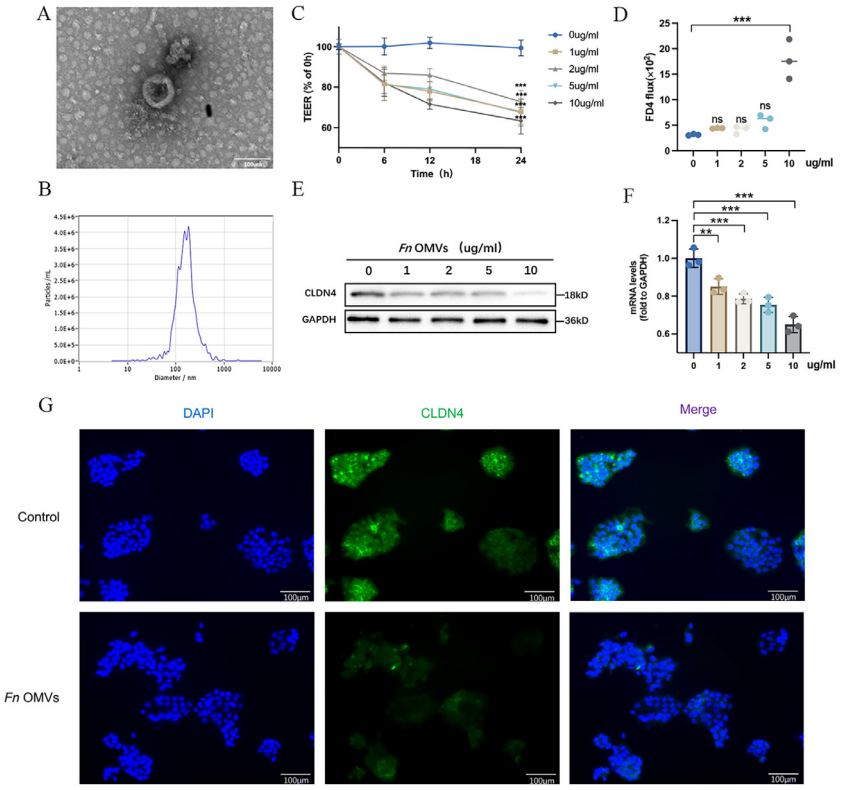

Fig. 3 – *F.n*-OMVs impair epithelial barrier integrity in HaCaT cells by downregulating Claudin-4 expression. (A) TEM image showing the typical cup-shaped morphology of purified *F.n*-OMVs. (B) NTA showing the particle size distribution of *F.n*-OMVs cantered around ~100 nm. (C) TEER values of HaCaT monolayers treated with increasing concentrations of *F.n*-OMVs (0, 1, 2, 5, and 10 μg/mL) at 6, 12, 18, and 24 hours. A significant time- and dose-dependent decrease was observed. (D) FITC-dextran permeability assay showing increased paracellular permeability after 24-hour OMV treatment, consistent with barrier disruption. (E, F) RT-qPCR and Western blot analyses of Claudin-4 expression showing dose-dependent downregulation at both mRNA and protein levels following *F.n*-OMVs treatment for 24 hours. (G) Immunofluorescence staining of Claudin-4 in HaCaT cells treated with *F.n*-OMVs (10ug/mL for 24 hours), showing reduced fluorescence intensity and disrupted membrane localization. Scale bar = 200 μm. *P < .05, **P < .01, ***P < .001.

supporting the critical role of epithelial junction disruption in the pathogenesis of OLP. However, these studies were largely based on bulk tissue analyses or immunohistochemical observations and did not resolve cell type specific expression patterns or investigate the upstream microbial or signalling mechanisms responsible for tight junction dysregulation. In contrast, the present study is the first to integrate spatial transcriptomics and single-cell sequencing technologies to precisely delineate the epithelial-specific and spatially resolved expression pattern of Claudin-4 in OLP lesions. Claudin-4 is a critical transmembrane tight junction protein that regulates paracellular permeability and ion selectivity, thereby playing a vital role in the maintenance and modulation of epithelial barrier function.[19] Loss of Claudin-4 expression can lead to increased mucosal permeability and facilitate the translocation of microbes and inflammatory mediators, ultimately exacerbating local tissue inflammation. Previous studies have demonstrated that in DSS-induced colitis mouse models, claudin-4 expression is significantly downregulated, accompanied by disrupted colonic architecture and impaired barrier function.[22,23] Similarly, in Caco-2 human colonic epithelial cells, TNF-α stimulation markedly reduces claudin-4 expression and decreases transepithelial electrical resistance (TEER), further supporting its essential role in epithelial barrier integrity.[22,23] Moreover, intratracheal administration of lipopolysaccharide (LPS) has been reported to induce distal intestinal inflammation associated with decreased Claudin-4 expression, epithelial barrier alteration, and goblet cell expansion, indicating that Claudin-4 downregulation can occur as a systemic epithelial response to inflammatory stimuli beyond the primary site of exposure.[24] These findings suggest that Claudin-4 downregulation is closely associated with epithelial barrier disruption in various chronic inflammatory diseases. Therefore, our findings suggest that the downregulation of Claudin-4 and the associated epithelial barrier dysfunction in OLP may reflect an underlying disturbance in mucosal barrier homeostasis, offering new mechanistic insights and directions for future research into the pathogenesis of OLP.

In addition to the observed downregulation of Claudin-4 expression in OLP tissues, we further investigated the potential role of pathogenic microorganisms in this process. Previous studies have shown that *F.nucleatum* , a conditionally pathogenic anaerobe, is significantly enriched in various mucosal-

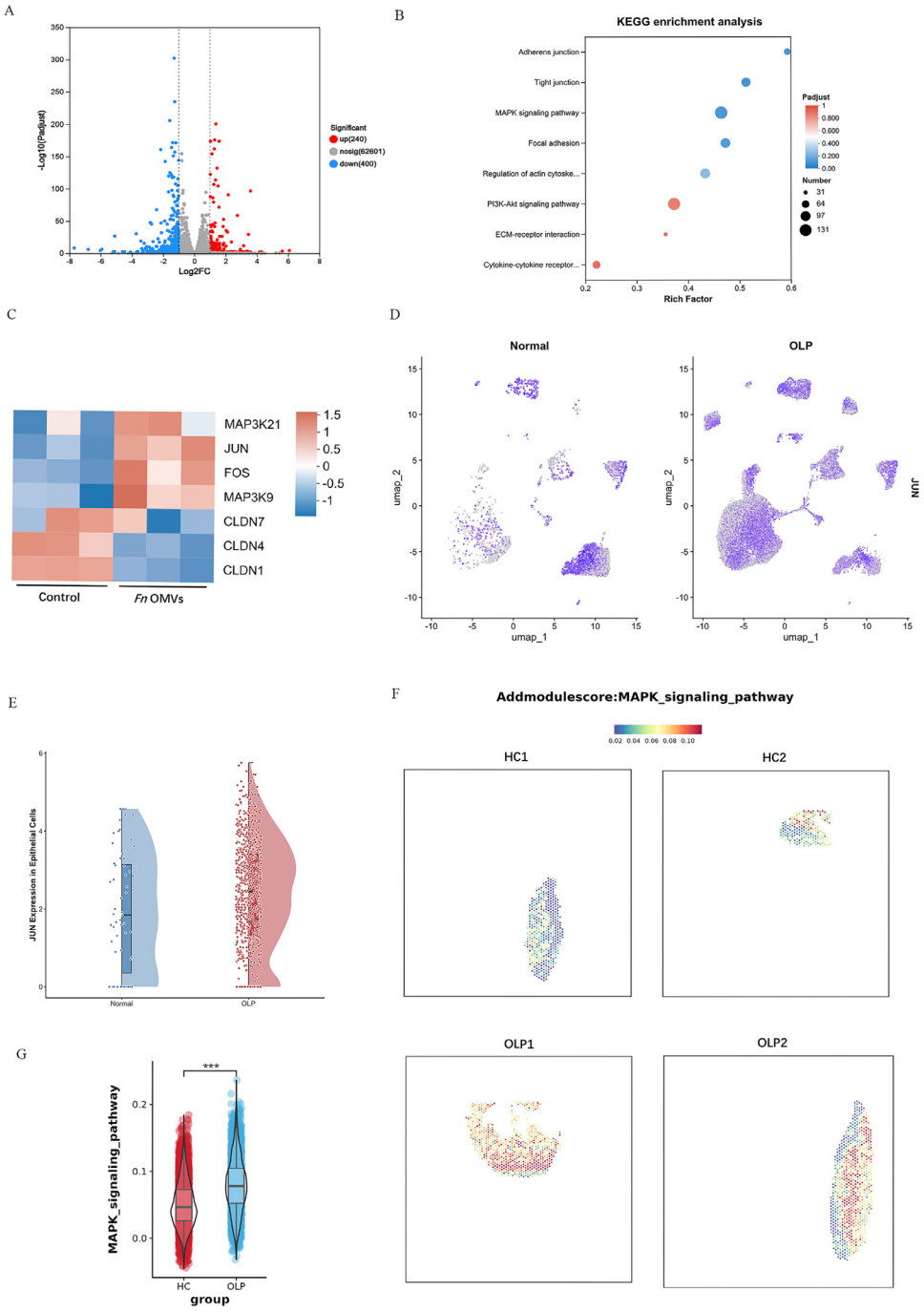

Fig. 4 – Multi-omics analyses identify the MAPK signalling pathway as a key mediator of *F.n*-OMVs-induced epithelial barrier disruption. (A) Volcano plot showing differentially expressed genes (DEGs) in HaCaT cells treated with *F.n*-OMVs (10 μg/mL, 24 hours) compared to untreated controls. (B) KEGG pathway enrichment analysis of DEGs. (C) Heatmap of representative DEGs showing upregulation of MAPK pathway genes (e.g., MAP3K21, MAP3K9, JUN, FOS) and downregulation of tight junction genes (CLDN1, CLDN4, CLDN7). (D, E) Single-cell RNA sequencing analysis revealed a significant upregulation of JUN expression in epithelial cell clusters. (F, G) Spatial transcriptomic analysis further confirmed significant activation of the MAPK signalling pathway in OLP tissues.

associated diseases, including inflammatory bowel disease (IBD), colorectal cancer, and oral squamous cell carcinoma.[10,25,26] Consistently, our previous research also identified a notable accumulation of *F.nucleatum* on the mucosal surface of OLP lesions,[7] suggesting that *F.nucleatum* may play an important role in the pathogenesis of OLP. Outer membrane vesicles (OMVs), nanoscale vesicles secreted by Gram-negative bacteria, are increasingly recognized as key mediators of host

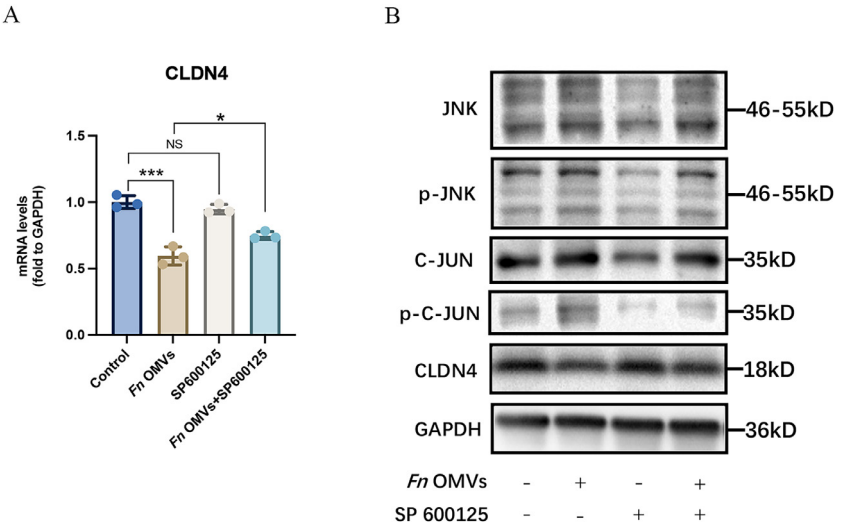

Fig. 5 – The JNK/c-JUN signalling pathway mediates *F.n*-OMVs-induced downregulation of Claudin-4 and disruption of epithelial barrier function in HaCaT cells. (A) qPCR results showed that *F.n*-OMVs significantly decreased Claudin-4 mRNA expression, which was markedly reversed by SP600125 pretreatment, indicating the involvement of the JNK pathway in Claudin-4 transcriptional repression. (B) Western blot analysis demonstrated that OMVs treatment significantly reduced Claudin-4 protein levels, while SP600125 pretreatment restored protein expression close to baseline. OMVs stimulation significantly increased the phosphorylation levels of JNK and its downstream transcription factor c-JUN, whereas SP600125 markedly inhibited their phosphorylation, confirming effective blockade of the signalling pathway. *P < .05, **P < .01, ***P < .001.

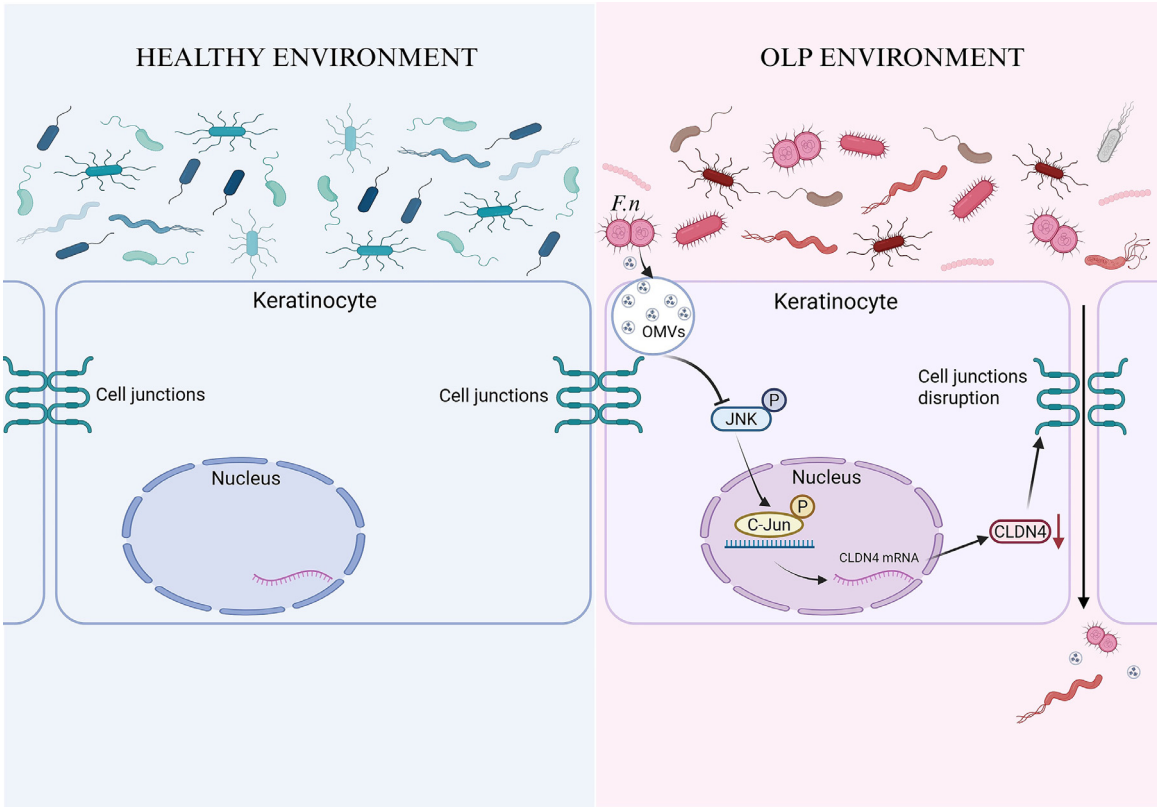

Fig. 6 – Schematic model illustrating epithelial barrier disruption induced by *F.n*-OMVs via the JNK/c-JUN/Claudin-4 axis. In the healthy oral epithelium, Claudin-4 is stably expressed, maintaining intact tight junctions and low paracellular permeability under basal JNK/c-JUN signaling activity. Upon exposure to *Fusobacterium nucleatum*-derived outer membrane vesicles (*F.n*-OMVs), JNK signaling is activated, leading to phosphorylation of c-JUN and suppression of Claudin-4 transcription. Reduced Claudin-4 expression disrupts tight junction organization, increases epithelial permeability, and may promote inflammatory responses in the underlying tissue microenvironment.

–microbe interactions. They not only contribute to interbacterial communication but also act as carriers of virulence factors, enabling bacteria to influence host cellular processes without direct contact.[27] Emerging evidence has demonstrated that OMVs derived from *Desulfovibrio fairfieldensis* and adherent-invasive *Escherichia coli*can impair intestinal barrier function by inhibiting the expression of tight junction proteins in human colonic epithelial cells.[28,29] Similarly, OMVs from *E. coli* BL21 significantly reduced E-cadherin expression in Caco-2 and HT-29 cells, compromising epithelial integrity and increasing permeability.[30] In this study, we provide the first evidence that *F.n*-OMVs directly target human oral keratinocytes, leading to a marked downregulation of Claudin-4 expression and disruption of epithelial barrier function. These findings not only align with previous reports on barrier dysfunction induced by pathogen-derived OMVs in other mucosal systems but also highlight a potentially pivotal role for *F.nucleatum* in OLP-associated barrier impairment. Furthermore, they emphasize the pathogenic potential of specific microbiome components within the oral ecosystem, offering novel insights into the contribution of microbial dysbiosis to OLP pathogenesis and providing a valuable entry point for future research into microbiota-mediated epithelial regulation.

Beyond their effects on epithelial cells, microbial components can reshape the inflammatory microenvironment through metabolic and mitochondrial reprogramming of immune cells. Zhan et al. showed that macrophage senescence in periodontitis is associated with enhanced glycolysis and increased CSF-1R expression, and that glycolytic inhibition attenuates inflammation.[31] Similarly, Liu et al. reported that lipoteichoic acid induces mitochondrial dysfunction in macrophages, characterized by disrupted dynamics, increased ROS production, and activation of NF-κB and Caspase-1; restoration of mitochondrial homeostasis mitigated the inflammatory response.[32]

Although the present study focuses on epithelial barrier disruption mediated by *F.n*- OMVs, these findings suggest that once barrier integrity is compromised, microbial products may access the lamina propria and further amplify mucosal inflammation through metabolic and mitochondrial regulation of resident immune cells.

We further elucidated the molecular mechanisms underlying epithelial barrier disruption induced by *F.n*-OMVs. JNK is the main kinase responsible for phosphorylating c-Jun, which acts as its key downstream target.[33] Previous studies have demonstrated that, following traumatic brain injury, endothelial S1pr2 expression is upregulated, leading to enhanced activation of the JNK/c-JUN pathway. This in turn promotes MMP-9 transcription, resulting in downregulation of the tight junction proteins ZO-1 and Occludin, and increased blood–brain barrier (BBB) permeability.[34] Similarly, WNT5B has been shown to compromise BBB integrity via activation of the JNK/c-JUN pathway, thereby reducing both mRNA and protein expression levels of ZO-1 in vitro and in vivo.[35] In addition, resveratrol, a natural compound with JNK-inhibitory activity, was reported to prevent the endocytosis and degradation of Claudin-4 and ZO-1, thereby attenuating deoxynivalenol (DON)-induced decreases in TEER and increases in FITC-dextran permeability.[36] Collectively, these findings suggest that the JNK/c-JUN pathway may represent a common regulatory mechanism for maintaining epithelial and endothelial barrier integrity. In the present study, we found that *F.n*-OMVs markedly activated the JNK/c-JUN signalling pathway and significantly downregulated Claudin-4 expression. Immunoblot analysis revealed elevated levels of phosphorylated JNK (p-JNK) and phosphorylated c-JUN (p–c-JUN), indicating activation of the pathway. Functional inhibition of JNK restored Claudin-4 expression and rescued epithelial barrier function in HaCaT cells, further supporting the notion that JNK/c-JUN pathway activation plays a critical role in mediating Claudin-4 suppression and epithelial barrier disruption.

Despite the novel findings and comprehensive multi-omics approach, several limitations should be acknowledged. First, although we demonstrated that *F.n*-OMVs impair epithelial barrier function through activation of the JNK/c-JUN signalling pathway in vitro, the current study lacks in vivo validation. Future studies using animal models or clinical samples from OLP patients would help to confirm the physiological relevance of these findings. Second, OMVs are known to contain a complex mixture of proteins, lipids, and nucleic acids; however, we did not characterize the specific components responsible for JNK/c-JUN pathway activation. Identifying the key virulence factors within OMVs would provide deeper mechanistic insights. Third, while our results show that inhibition of the JNK pathway reverses Claudin-4 downregulation, other signalling pathways may also contribute to the observed epithelial barrier disruption and warrant further investigation. Lastly, the use of a single keratinocyte cell line (HaCaT) may limit the generalizability of our findings, therefore, validation in primary oral epithelial cells or organotypic models would strengthen the conclusions.

In summary, our study not only expands the current understanding of epithelial barrier disruption in OLP, but also elucidates the molecular mechanism by which pathogen-derived OMVs mediate changes in key tight junction proteins via the JNK/c-JUN signalling pathway. These findings provide a critical theoretical basis and valuable direction for future investigations into microbiota-mediated barrier regulation and its role in chronic inflammatory diseases of the oral mucosa.

Funding

This work was supported by the National Natural Science Foundation of China (82101008,82203551) and an Intrahospital Research Grant (2022yxyjxys).

Author contributions

Ruru Shao: Study design, experimental implementation, manuscript writing. Zhenyuan Wang: Experimental implementation, manuscript revision. Chenglong Yang: Bioinformatics analysis, manuscript revision. Junjun Chen: Manuscript review and revision. Guanhuan Du: Manuscript review and revision, funding acquisition.

Declaration of competing interest

None disclosed.

REFERENCES

1. Louisy A, Humbert E, Samimi M. Oral lichen planus: an update on diagnosis and management. Am J Clin Dermatol 2024;25(1):35–53. doi: 10.1007/s40257-023-00814-3.
2. Nosratzehi T. Oral lichen planus: an overview of potential risk factors, biomarkers and treatments. Asian Pac J Cancer Prev. 2018;19(5):1161–7. doi: 10.22034/apjcp.2018.19.5.1161.
3. Lin D, Yang L, Wen L, Lu H, Chen Q, Wang Z. Crosstalk between the oral microbiota, mucosal immunity, and the epithelial barrier regulates oral mucosal disease pathogenesis. Mucosal Immunol 2021;14(6):1247–58. doi: 10.1038/s41385-021-00413-7.
4. Yan L, Xu J, Lou F, et al. Alterations of oral microbiome and metabolic signatures and their interaction in oral lichen planus. J Oral Microbiol 2024;16(1):2422164. doi: 10.1080/20002297.2024.2422164.
5. Yu FY, Wang QQ, Li M, et al. Dysbiosis of saliva microbiome in patients with oral lichen planus. BMC Microbiol 2020;20(1):75. doi: 10.1186/s12866-020-01733-7.
6. Ju HM, Ahn YW, Ok SM, Jeong SH, Na HS, Chung J. Microbial profiles in oral lichen planus: comparisons with healthy controls and erosive vs. non-erosive subtypes. Diagnostics (Basel) 2024;14(8). doi: 10.3390/diagnostics14080828.
7. Du G, Deng Y, Pan L, Han X, Tang G, Yu S. Preliminary analysis of mucosal and salivary bacterial communities in oral lichen planus. Oral Dis 2023;29(7):2710–22. doi: 10.1111/odi.14493.
8. Brennan CA, Garrett WS. Fusobacterium nucleatum - symbiont, opportunist and oncobacterium. Nat Rev Microbiol 2019;17(3):156–66. doi: 10.1038/s41579-018-0129-6.
9. Sartorio MG, Pardue EJ, Feldman MF, Haurat MF. Bacterial outer membrane vesicles: from discovery to applications. Annu Rev Microbiol 2021;75:609–30. doi: 10.1146/annurev-micro-052821-031444.
10. Zheng X, Gong T, Luo W, et al. Fusobacterium nucleatum extracellular vesicles are enriched in colorectal cancer and facilitate bacterial adhesion. Sci Adv 2024;10(38):eado0016. doi: 10.1126/sciadv.ado0016.
11. Hong M, Li Z, Liu H, et al. Fusobacterium nucleatum aggravates rheumatoid arthritis through FadA-containing outer membrane vesicles. Cell Host Microbe 2023;31(5) 798-810.e7. doi: 10.1016/j.chom.2023.03.018.
12. Liu L, Liang L, Yang C, Zhou Y, Chen Y. Extracellular vesicles of Fusobacterium nucleatum compromise intestinal barrier through targeting RIPK1-mediated cell death pathway. Gut Microbes 2021;13(1):1–20. doi: 10.1080/19490976.2021.1902718.
13. Chen G, Gao C, Jiang S, et al. Fusobacterium nucleatum outer membrane vesicles activate autophagy to promote oral cancer metastasis. J Adv Res 2024;56:167–79. doi: 10.1016/j.jare.2023.04.002.
14. Zhang L, Zhang D, Liu C, et al. Outer membrane vesicles derived from fusobacterium nucleatum trigger periodontitis through host overimmunity. Adv Sci (Weinh) 2024;11(47):e2400882. doi: 10.1002/advs.202400882.
15. Williams DW, Greenwell-Wild T, Brenchley L, et al. Human oral mucosa cell atlas reveals a stromal-neutrophil axis regulating tissue immunity. Cell 2021;184(15) 4090-104.e15. doi: 10.1016/j.cell.2021.05.013.
16. Choi YS, Kim Y, Yoon HJ, et al. The presence of bacteria within tissue provides insights into the pathogenesis of oral lichen planus. Sci Rep 2016;6:29186. doi: 10.1038/srep29186.
17. Qing M, Yang D, Shang Q, et al. CD8(+) tissue-resident memory T cells induce oral lichen planus erosion via cytokine network. Elife 2023;12. doi: 10.7554/eLife.83981.
18. Hämäläinen L, Soini Y, Pasonen-Seppänen S, Siponen M. Alterations in the expression of EMT-related proteins claudin-1, claudin-4 and claudin-7, E-cadherin, TWIST1 and ZEB1 in oral lichen planus. J Oral Pathol Med 2019;48(8):735–44. doi: 10.1111/jop.12917.
19. Günzel D, Yu AS. Claudins and the modulation of tight junction permeability. Physiol Rev 2013;93(2):525–69. doi: 10.1152/physrev.00019.2012.
20. Yang M, Liu X, Luo Q, Xu L, Chen F. An efficient method to isolate lemon derived extracellular vesicles for gastric cancer therapy. J Nanobiotechnology 2020;18(1):100. doi: 10.1186/s12951-020-00656-9.
21. Ren X, Li K, Fang X, et al. Oral mucosal changes in tight junction proteins in patients with oral lichen planus. Oral Dis 2024;30(7):4367–75. doi: 10.1111/odi.14912.
22. Cai L, Li X, Geng C, Lei X, Wang C. Molecular mechanisms of somatostatin-mediated intestinal epithelial barrier function restoration by upregulating claudin-4 in mice with DSS-induced colitis. Am J Physiol Cell Physiol 2018;315(4) C527-c36. doi: 10.1152/ajpcell.00199.2018.
23. Li Y, Li X, Geng C, Guo Y, Wang C. Somatostatin receptor 5 is critical for protecting intestinal barrier function in vivo and in vitro. Mol Cell Endocrinol 2021;535:111390. doi: 10.1016/j.mce.2021.111390.
24. McQuade RM, Bandara M, Diwakarla S, et al. Gastrointestinal consequences of lipopolysaccharide-induced lung inflammation. Inflamm Res 2023;72(1):57–74. doi: 10.1007/s00011-022-01657-0.
25. Nie F, Zhang J, Tian H, et al. The role of CXCL2-mediated crosstalk between tumor cells and macrophages in Fusobacterium nucleatum-promoted oral squamous cell carcinoma progression. Cell Death Dis 2024;15(4):277. doi: 10.1038/s41419-024-06640-7.
26. Wang Z, Li B, Bao L, et al. Fusobacterium nucleatum aggravates intestinal barrier impairment and colitis through il-8 induced neutrophil chemotaxis by activating epithelial cells. J Inflamm Res 2024;17:8407–20. doi: 10.2147/jir.S470376.
27. Li M, Zhou H, Yang C, et al. Bacterial outer membrane vesicles as a platform for biomedical applications: an update. J Control Release 2020;323:253–68. doi: 10.1016/j.jconrel.2020.04.031.
28. Nadalian B, Nadalian B, Zali MR, Yadegar A. Outer membrane vesicles derived from adherent-invasive escherichia coli induce inflammatory response and alter the gene expression of junction-associated proteins in human intestinal epithelial cells. Can J Infect Dis Med Microbiol 2024;2024:2701675. doi: 10.1155/2024/2701675.
29. Nie Y, Xie XQ, Zhou L, et al. Desulfovibrio fairfieldensis-derived outer membrane vesicles damage epithelial barrier and induce inflammation and pyroptosis in macrophages. Cells 2022;12(1). doi: 10.3390/cells12010089.
30. Vanaja SK, Russo AJ, Behl B, et al. Bacterial outer membrane vesicles mediate cytosolic localization of lps and caspase-11 activation. Cell 2016;165(5):1106–19. doi: 10.1016/j.cell.2016.04.015.
31. Zhan J, Kang J, Wei Y, et al. Pexidartinib inhibits macrophage senescence through glycolysis in periodontitis microenvironment. Int Dent J 2025;75(4):100843. doi: 10.1016/j.identj.2025.100843.
32. Liu S, Liu X, Li G, Liu H, Zhang W, Pan S. Lipoteichoic acid stimulation of macrophages causes mitochondrial dysfunction. Int Dent J 2026;76(1):109290. doi: 10.1016/j.identj.2025.109290.
33. Kumar A, Singh UK, Kini SG, et al. JNK pathway signaling: a novel and smarter therapeutic targets for various biological diseases. Future Med Chem 2015;7(15):2065–86. doi: 10.4155/fmc.15.132.
34. Cheng H, Men Y, An Y, et al. Overexpression of endothelial S1pr2 promotes blood-brain barrier disruption via JNK/c-Jun/MMP-9 pathway after traumatic brain injury in both in vivo and in vitro models. Front Pharmacol 2024;15:1448570. doi: 10.3389/fphar.2024.1448570.

35. Qu X, Yang R, Tan C, Chen H, Wang X. Astrocytes-secreted WNT5B disrupts the blood-brain barrier via ROR1/JNK/c-JUN cascade during meningitic escherichia coli infection. Mol Neurobiol 2025;62(1):661–73. doi: 10.1007/s12035-024-04303-4.

36. Li E, Horn N, Ajuwon KM. Mechanisms of deoxynivalenol-induced endocytosis and degradation of tight junction proteins in jejunal IPEC-J2 cells involve selective activation of the MAPK pathways. Arch Toxicol 2021;95(6):2065–79. doi: 10.1007/s00204-021-03044-w.